Dalton Transactions

PAPER

View Article Online
View Journal | View Issue

Cite this: *Dalton Trans.*, 2025, **54**, 16864

Metallocarbonyl bromomaleimide derivatives for thiol bioconjugation and disulfide bridging: spectroscopic and biological properties

Karolina Koprowska, [a,b] Nathalie Fischer-Durand, [c] Sylwia Michlewska, [d] Magdalena Gapińska, [d] Marika Grodzicka, [d] Anna Makal, [e] Joanna Krzeszczakowska, [e] Anna Wrona-Piotrowicz, [a] Laurent Lignières, [f] Michèle Salmain [c] and Bogna Rudolf *[a]

Received 4th October 2025,
Accepted 27th October 2025

DOI: 10.1039/d5dt02375k

rsc.li/dalton

Mono- and dibromomaleimides have been introduced as useful reagents for the modification of cysteine residues, disulfide rebridging and peptide stapling. Herein, we investigate the reaction of the organometallic compounds $CpFe(CO)_2(\eta^1$-2-bromomaleimidato) and $CpFe(CO)_2(\eta^1$-2,3-dibromomaleimidato) and their organic analogs 2-bromomaleimide and 2,3-dibromomaleimide with the bioactive thiols *N*-acetyl cysteine methyl ester and 1-thio-β-D-glucose tetraacetate, along with the disulfide-containing protein bovine insulin. Substitution and/or addition products were isolated and characterized by NMR, IR and MS and the molecular structure of two reaction products was confirmed by X-ray diffraction. In the case of the organic derivatives, formation of the dithiomaleimide adducts was also assessed by the emission of fluorescence in the green region. Visible light irradiation of the metallocarbonyl dithiomaleimides resulted in the decomposition of the organometallic fragment and generation of fluorescent products. This feature greatly helped to delineate the transformations operated by the metallocarbonyl compounds within cancer cells and provided clues to their molecular mechanism of action.

Introduction

As Michael acceptors, maleimides are extensively used for conjugation of protein thiols, allowing a wide variety of functions to be site-selectively introduced, given the relatively low abundance of free cysteines in proteins and their high nucleophilicity.[1] For proteins lacking solvent-accessible free cysteines, disulfides formed by bridging between two cysteines afford an attractive alternative for site-selective bioconjugation[2] and disulfide rebridging methods with appropriate reagents form the basis of the synthesis of homogeneous antibody–drug conjugates (ADCs).[3,4]

In this context, (di)bromomaleimides ((D)BM) were initially introduced by Baker and Caddick as useful reagents for the reversible modification of cysteine residues.[5] By extension, mono- and dibromomaleimides allowed for the rebridging of disulfide bonds in peptides and proteins through reduction followed by substitution and addition or double substitution, respectively.[6–9] DBMs have also been employed for the stapling of peptides carrying cysteines at the i and $i + 4$ positions to constrain them into α-helical conformation.[10,11] Therefore, the unique reactivity of (di)bromomaleimides provides a general route for the labeling of thiol and/or disulfide containing peptides and proteins, and the synthesis of homogenous antibody–drug conjugates[12–14] by taking advantage of the N atom of the maleimide ring as a point of attachment of various functionalities. Another attractive feature of DBMs is the generally strong emission properties of the dithiomaleimide (DTM) products in the green region, providing convenient assessment of thiol conjugation or disulfide rebridging.[15–19] For instance, the reversible functionalization of DTM-containing thermoresponsive polymers was reported based on sequential thiol-exchange reactions that allowed tuning the lower critical solution temperature (LCST) and fluorescent properties of the polymers according to the thiols appended to the maleimide scaffolds.[20]

[a]*University of Lodz, Faculty of Chemistry, Department of Organic Chemistry, 91-403 Lodz, Poland. E-mail: bogna.rudolf@chemia.uni.lodz.pl*
[b]*University of Lodz, Bio-Med-Chem Doctoral School of University of Lodz and Lodz Institutes of The Polish Academy of Sciences, 90-237 Lodz, Poland*
[c]*Sorbonne Université, CNRS, Institut Parisien de Chimie Moléculaire (IPCM), 4 place Jussieu, 75005 Paris, France*
[d]*University of Lodz, Faculty of Biology and Environmental Protection, Laboratory of Microscopic Imaging and Specialized Biological Techniques, Banacha St. 12/16, Lodz 90-237, Poland*
[e]*Biological and Chemical Research Centre, Faculty of Chemistry, University of Warsaw, Żwirki I Wigury 101, 02-089 Warszawa, Poland*
[f]*Sorbonne Université, CNRS, FCMol, UAR 2769, 4 place Jussieu, 75005 Paris, France*

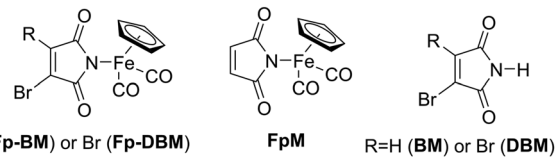

Fig. 1 Structure of mono- and dibromomaleimides **Fp-BM** and **Fp-DBM**, the organic analogs **BM** and **DBM** and the non brominated Fp-maleimide **FpM**.

In 2012, we reported the synthesis and characterization of (η^5-cyclopentadienyl) iron dicarbonyl (abbreviated Fp) complexes **Fp-BM** and **Fp-DBM** containing an η^1-bromo- or dibromomaleimidato ligand, Fig. 1.[21] According to LC-MS analysis, both complexes formed adducts with cysteine or the cysteine-containing tripeptide glutathione *via* substitution of one or two bromides and/or addition to the double bond of the maleimide ring. On the other hand, Fp-maleimide (**FpM**, Fig. 1) was reported to release its 2 CO, cyclopentadiene and maleimide under visible light irradiation, thus acting as a photoCORM.[22] **FpM** was also shown to decrease the viability of HL-60 cells (human promyelocytic leukemia) at high concentration, induce DNA damage and stimulate HO-1 gene expression in a concentration-dependent manner. However, no clear correlation between visible light irradiation and biological effects could be drawn from these experiments.[23]

Herein we report a thorough investigation of the reaction of compounds **Fp-BM** and **Fp-DBM** and their organic analogs **BM** and **DBM** (Fig. 1) with cysteine and glucose derivatives, as well as the disulfide-containing protein bovine insulin. Reaction products were isolated and characterized by a range of spectroscopic methods. Stability in physiological buffer and effect of visible light irradiation on the organometallic DTM were studied. Eventually, the ability of the organic and organometallic DBM and DTM to lower the viability of "triple negative" human breast cancer cells MDA-MB-231 was investigated and confocal microscopy experiments were performed to detect the presence of fluorescent compounds in these cells and provide useful information on the mechanism of transformation of the organometallic compounds.

Experimental

General procedures

Cyclopentadienyliron(II) dicarbonyl dimer, 2,3-dibromomaleimide, *N*-acetyl cysteine methyl ester, 1-thio-β-D-glucose tetraacetate and bovine insulin were purchased from Sigma-Aldrich (Merck). **BM** and $CpFe(CO)_2I$ were synthesized as previously described.[5,24] **Fp-BM** and **Fp-DBM** were synthesized following previously published method, by photochemical reaction of $CpFe(CO)_2I$ with 2-bromomaleimide or 2,3-dibromomaleimide in the presence of diisopropyl amine in toluene.[21] Methanol and toluene were purchased from POCH (Polish Chemical Reagents), and used as solvents without further purification. All syntheses were carried out under argon.

Flash chromatography was performed on silica gel 60 (Merck, 40–63 mm). Protein solutions were concentrated and buffer exchanged using Vivaspin 6 (3 kDa, Sartorius) or Amicon Ultra-15 (3 kDa, Millipore) centrifugal filter devices with a Megafuge ST Plus series centrifuge (Thermo Scientific). UV/Vis spectra were recorded on Cary 50 (Varian) or Lambda 45 spectrophotometers (PerkinElmer). NMR spectra were recorded on Bruker Avance 300, Avance 400 and Avance 600 spectrometers. NMR spectra were collected in $CDCl_3$, CD_2Cl_2, MeOD or DMSO-d_6. The chemical shifts are stated in part per million (ppm). Coupling constants are calculated in Hertz (Hz). Fluorescence spectra were recorded on a FP-6200 spectrofluorimeter equipped with an ETC-272T temperature controller (Jasco) or a LS55 Fluorimeter (PerkinElmer). Electrospray ionization mass spectrometry (ESI-MS) spectra were recorded on Varian 500-MS LC ion trap spectrometer. HRMS spectra in positive mode were obtained on an ESI-LTQ Orbitrap XL from Thermo Fisher Scientific (Waltham, MA, USA) coupled to an Agilent 1100 HPLC (Santa Clara, CA, USA) for FIA (flow injection analysis) injection. Infrared (IR) spectra of KBr pellets were recorded on a Fourier Transform InfraRed (FTIR) NEXUS (Thermo Nicolet) spectrometer.

LC-MS analysis

Intact protein conjugates samples were injected in normal mode onto a Luna C18 reverse phase column (100 Å, 3 μm, 1.0 mm × 150 mm) from Phenomenex (Torrance, CA, USA) using an UltiMate 3000 HPG-3400RS chromatographic system from Thermo Fisher Scientific (Waltham, MA, USA). Mobile phases A and B were respectively H_2O and MeCN, both acidified with 0.1% FA (Formic Acid). The samples were eluted at a flow rate of 70 μL min^{-1} using the following 15 min gradient: 0–5 min hold at 5% B, 5–8 min slope until 60% B, 8–10 min slope until 80% B followed by a washing step of 1 min at 80% B, then an equilibration step of 4 min at 5% B is done. Chromatographic system was hyphenated to a Q-Trap API 2000 mass spectrometer from AB Sciex (Marlborough, MA, USA). Ionization process occurs using the conventional ESI ion source of the instrument, operating in the positive ion polarity in Enhanced MS scans profile mode. MS spectra were acquired with a mass range of m/z 100–1700 and a cycle time of 1.8 s. The scan rate was fixed at 1000 Da per s. The voltage of the Ion spray source was fixed at 5500 V, 15 psig of ion source gas, 15 psig of curtain gas and a high collision gas level (all with N_2 gas supply). The declustering potential was applied at 80.0 V, the entrance potential at 10.0 V and the collision energy at 10 eV.

Deconvolution of mass spectra

Deconvolution steps were done using UniDec software (GUI 6.0.4 version).[25] For the data processing part, the following parameters were applied: mass range at m/z 900–1700; background subtraction with a Gaussian smoothing at 10; subtracted curved at 200 and data normalization. For the deconvolution step, the following parameters were used: charge range 1–20; mass range 5 000–10 000 Da; sample mass every 1 Da;

smoothing of charge states distribution; no suppression of artifacts; 500 maximum number of iterations, with a *m*/*z* to mass transformation in smart mode. For peak selection and plotting, the following parameters were applied: peak detection range at 50.0 Da; peak detection threshold at 0.01 in reconvolved/profile mode; peak normalization at Max.

FT-IR spectra of nitrocellulose membranes

Spectra were recorded on a benchtop Bruker Tensor 27 IR spectrometer equipped with a DTGS detector, and a 6 mm-diameter membrane holder perpendicularly positioned with respect to the IR beam. FT-IR spectra were recorded and manipulated on a Windows-operating PC using the OPUS 6.5 software. Routinely, 44 scans were coadded in 40 seconds and the resulting interferogram was apodized using a Blackman-Harris 3-Term function and then Fourier-transformed to yield a 4 cm^{-1} resolution spectrum. Qualitative analysis of Fp entities in insulin conjugate solutions was carried out as follows: the conjugate was diluted in 20 mM $AcONH_4$ and 4 μL in duplicate were spotted onto nitrocellulose membranes. A blank membrane was prepared by spotting 4 μL of 20 mM $AcONH_4$. Membranes were dried for at least 2 h at room temperature in the dark before IR recording in the range 1800 and 2200 cm^{-1}.

Synthesis of TM-Cys

N-Acetyl-L-cysteine methyl ester (50 mg, 0.282 mmol) and NaOAc (23.1 mg, 0.282 mmol) were dissolved in methanol (3 mL) and **BM** (54.6 mg, 0.31 mmol) was added in methanol (3 mL). The reaction mixture was stirred at room temperature for 30 min then solvent was removed *in vacuo* and product was purified by flash chromatography on silica gel (AcOEt) to afford **TM-Cys** as a white solid (70 mg, 93% yield). ^{1}H NMR (600 MHz, CD_3OD) δ 6.34 (s, 1H, C═CH), 4.77 (dd, 1H, J_1 = 9.0 Hz, J_2 = 6.0 Hz, C<u>H</u>–NH), 3.77 (s, 3H, OC<u>H</u>$_3$), 3.51 (dd, 1H, J_1 = 6.0 Hz, J_2 = 15 Hz, S–C<u>H</u>$_2$), 3.32 (m, 1H, S–C<u>H</u>$_2$), 1.99 (s, 3H, C<u>H</u>$_3$); ^{13}C NMR (150 MHz, CD_3OD) δ 172.1, 170.7, 170.2, 169.0 (C═O), 150.3 (C═C), 119.4 (C═C–S), 51.8 (OCH_3), 50.9 (HC–NH), 32.2 (H_2C–S), 20.9 (CH_3); IR (solid, cm^{-1}): 3312 (νN–H), 1754, 1710 (νC═O), 1687, 1655 (νC═C); HRMS (ES^+) *m*/*z* calculated for $C_{10}H_{12}N_2O_5SH$ $(M + H)^+$ 273.0540, found 273.0540.

Synthesis of DTM-Cys

N-Acetyl-L-cysteine methyl ester (0.195 g, 1.1 mmol) and NaOAc (90.1 mg, 1.1 mmol) were dissolved in methanol (5 mL) and **DBM** (0.127 g, 0.5 mmol) was added in methanol (5 mL). The reaction mixture was stirred at room temperature for 20 min then solvent was removed *in vacuo* and product was purified by flash chromatography on silica gel (AcOEt/MeOH, 95 : 5) to afford **DTM-Cys** as a yellow solid (0.19 g, 85%). ^{1}H NMR (600 MHz, DMSO-d^6) δ 8.46 (d, 2H, J = 7.8 Hz, 2xNH), 4.50 (td, 2H, J_1 = 8.4 Hz, J_2 = 5.4 Hz 2xC<u>H</u>-NH), 3.72 (dd, 1H, J_1 = 13.5 Hz, J_2 = 5.1 Hz, S–C<u>H</u>$_2$), 3.63 (s, 6H, 2xOC<u>H</u>$_3$), 3.41 (dd, 1H, J_1 = 13.5 Hz, J_2 = 8.7 Hz, S–C<u>H</u>$_2$), 1.84 (s, 6H, 2xC<u>H</u>$_3$); ^{13}C NMR (150 MHz, DMSO-d^6) δ 171.0, 169.9, 167.6 (C═O), 136.5 (C–S), 52.8 (OCH_3), 52.7 (HC–NH), 32.4 (H_2C–S), 22.7, 22.7 (CH_3); IR (KBr, cm^{-1}): 3382, 3344 (νN–H), 2958, 2926 (νC–H), 1768, 1725 (νC═O), 1674, 1648 (νC═C); HRMS (ES^+) *m*/*z* calculated for $C_{16}H_{21}N_3O_8S_2Na$ $(M + H)^+$ 470.0662, found 470.066.

Synthesis of Fp-TM-Cys

N-acetyl-L-cysteine methyl ester (53.2 mg, 0.30 mmol) and NaOAc (24.6 mg, 0.30 mmol) were dissolved in MeOH (5 mL) and **Fp-BM** (0.1 g, 0.27 mmol) was added in MeOH (10 mL). The reaction mixture was stirred at room for 24 h, then H_2O (100 mL) was added and the reaction mixture was extracted with AcOEt (3 × 100 mL). Combined organic layers were dried over $MgSO_4$. After evaporation of the solvent *in vacuo*, the crude product was purified by flash chromatography on silica gel (AcOEt/MeOH 95 : 5) to afford **Fp-TM-Cys** as a yellow oil (62 mg, 73%, *limited stability*). ^{1}H NMR (400 MHz, CD_2Cl_2) δ 6.39 (d, 1H, J = 6.4 Hz, NH), 6.21 (s, 1H, C═C<u>H</u>), 5.06 (s, 5H, Cp), 4.82 (td, 1H, J_1 = 5.4 Hz, J_2 = 4.1 Hz, C<u>H</u>–NH), 3.74 (s, 3H, OC<u>H</u>$_3$), 3.35 (dd, 1H, J_1 = 10.2 Hz, J_2 = 3.9 Hz, S–C<u>H</u>$_2$), 3.24 (dd, 1H, J_1 = 10.2 Hz, J_2 = 4.2 Hz, S–C<u>H</u>$_2$), 1.96 (s, 3H, C<u>H</u>$_3$); ^{13}C NMR (75 MHz, CD_2Cl_2) δ 212.3 (C≡O), 181.3, 179.4, 170.5, 169.7 (C═O), 151.6 (C═<u>C</u>–S), 124.4 (C═<u>C</u>–H), 85.0 (Cp), 52.8 (HC–NH), 51.3 (OCH_3), 33.5 (H_2C–S), 22.8 (CH_3); FTMS + ESI *m*/*z* calculated for $C_{17}H_{16}N_2O_7SFeH$ (MH^+) 449.0106, found 449.0133.

Synthesis of Fp-DTS-Cys

N-Acetyl-L-cysteine methyl ester (52.8 mg, 0.298 mmol) and NaOAc (24.4 mg, 0.298 mmol) were dissolved in MeCN (2 mL) and Fp-BM (50 mg, 0.142 mmol) was added in MeCN (2 mL). The reaction mixture was stirred at room temperature for 3 h then at 30 °C for 22 h. Cysteine (25 mg, 0.142 mmol) and NaOAc (11.6 mg, 0.142 mmol) were then added and the reaction mixture was stirred for 45 h at 30 °C. Solvent was removed *in vacuo* and products were purified by flash chromatography on silica gel (AcOEt/MeOH 95 : 5) to afford two diastereoisomers **Fp-DTS-Cys-a** and **Fp-DTS-Cys-b** as yellow solids (50.3 mg and 23.1 mg, 68.5 : 31.5, 93%).

Fp-DTS-Cys-a ^{1}H NMR (300 MHz, CD_2Cl_2) δ 7.75 (d, 1H, J = 8.1 Hz, NH), 7.14 (d, 1H, J = 7.5 Hz, NH), 5.07 (s, 3H, Cp), 5.06 (s, 2H, Cp), 4.88 (dt, 1H, J_1 = 8.1 Hz, J_2 = 4.8 Hz, C<u>H</u>–NH), 4.73 (td, 1H, J_1 = 7.5 Hz, J_2 = 4.5 Hz, C<u>H</u>–NH), 3.74 (s, 3H, OC<u>H</u>$_3$), 3.73 (s, 3H, OC<u>H</u>$_3$), 3.51 (s, 1H, S–C<u>H</u>$_{Su}$), 3.47 (s, 1H, S–C<u>H</u>$_{Su}$), 3.37 (m, 2H, S–C<u>H</u>$_2$), 3.04 (m, 2H, S–C<u>H</u>$_2$), 2.01 (s, 6H, C<u>H</u>$_3$); ^{13}C NMR (75 MHz, CD_2Cl_2) δ 212.3, 212.2 (C≡O), 186.8, 186.3, 171.1, 170.9, 170.1, 170.1 (C═O), 85.2 (Cp), 52.9 (C–C), 52.5 (OCH_3), 50.4 (HC–NH), 35.8, 34.0 (H_2C–S), 22.7, 22.6 (CH_3); IR (KBr, cm^{-1}): 2958, 2925 (νC–$H_{aliphat}$), 2046, 1997 (νC≡O), 1741 (νC═O), 1638 (νC═C); HRMS (ES^+) *m*/*z* calculated for $C_{23}H_{27}FeN_3O_{10}S_2Na$ $(M + Na)^+$ 648.0379, found 648.0378.

Fp-DTS-Cys-b ^{1}H NMR (300 MHz, CD_2Cl_2) δ 7.74 (d, J = 7.5 Hz, 1H, NH), 7.03 (d, J = 6.6 Hz, 1H, NH), 5.06 (s, 5H, Cp), 4.83 (m, 1H, C<u>H</u>–NH), 4.75 (m, 1H, C<u>H</u>–NH), 4.08 (d, J = 8.1 Hz, 1H, S–C<u>H</u>$_{Su}$), 4.00 (d, J = 8.1 Hz, 1H, S–C<u>H</u>$_{Su}$), 3.74 (s, 3H, OC<u>H</u>$_3$), 3.73 (s, 3H, OC<u>H</u>$_3$), 3.30 (m, 2H, S–C<u>H</u>$_2$), 3.04 (m, 2H, S–C<u>H</u>$_2$), 2.04 (s, 6H, C<u>H</u>$_3$); ^{13}C NMR (75 MHz, CD_2Cl_2) δ 212.3 (C≡O), 187.3, 186.7, 171.1, 170.3 (C═O), 85.3 (Cp), 52.6, 52.5 (OCH_3),

52.0 (HC–NH), 50.9, 49.2 (HC–CH), 35.7, 34.3 (H_2C–S), 22.7, 22.6 (CH_3); HRMS (ES^+) *m/z* calculated for $C_{23}H_{27}FeN_3O_{10}S_2Na$ $(M + Na)^+$ 648.0379, found 648.0381.

Synthesis of Fp-DTM-Cys

N-Acetyl-L-cysteine methyl ester (44.7 mg, 0.25 mmol) and NaOAc (20.6 mg, 0.25 mmol) were dissolved in MeCN (2 mL) and **Fp-DBM** (50 mg, 0.12 mmol) was added in MeCN (2 mL). The reaction mixture was stirred at room temperature for 2 h then at 30 °C overnight. Cysteine (10.6 mg, 0.125 mmol) and NaOAc (4.9 mg, 0.06 mmol) were then added and the reaction mixture was stirred for 24 h at 30 °C. Solvent was removed *in vacuo* and product was purified by flash chromatography on silica gel (CH_2Cl_2/MeOH 98 : 2) to afford **Fp-DTM-Cys** as a yellow orange solid (39 mg, 70%). ^{1}H NMR (300 MHz, CD_2Cl_2) δ 7.14 (d, J = 7.8 Hz, 2H, NH), 5.09 (s, 5H, Cp), 4.82 (dt, 2H, J_1 = 7.5 Hz, J_2 = 4.9 Hz, C$\underline{H}$–NH), 3.71 (s, 6H, OC$\underline{H}_3$), 3.68 (d, J = 5.1 Hz, 4H, S–C$\underline{H}_2$), 1.99 (s, 6H, C$\underline{H}_3$); ^{13}C NMR (75 MHz, CD_2Cl_2) δ 212.9, 212.6 (C≡O), 177.5, 171.2, 169.8 (C=O), 140.1 (C=C), 85.2 (Cp), 53.1 (OCH_3), 52.6 (HC–NH), 33.5 (H_2C–S), 22.5 (CH_3); IR (KBr, cm^{-1}): 2958, 2927 (νC–H) 2045, 1995 (νC≡O), 1742 (νC=O), 1645 (νC=C); HRMS (ES^+) *m/z* calculated for $C_{23}H_{25}FeN_3O_{10}S_2H$ $(M + H)^+$ 624.043, found 624.0409.

Synthesis of DTM-Gluc

Thioglucose tetraacetate (0.4 g, 1.1 mmol) and NaOAc (90.2 mg, 1.1 mmol) were dissolved in methanol (6 mL) and **DBM** (0.127 g, 0.5 mmol) was added in methanol (6 mL). The reaction mixture was stirred at room temperature for 10 min. Methanol was removed *in vacuo* and the residue was diluted in CH_2Cl_2 (20 mL) and H_2O (20 mL). The aqueous layer was extracted with CH_2Cl_2 (3 × 30 mL) and the combined organic layers were dried over anhydrous Na_2SO_4. The crude material was further purified by flash chromatography on silica gel (CH_2Cl_2/MeOH, 98 : 2) to afford **DTM-Gluc** as a yellowish-green solid (0.39 g, yield 95%). ^{1}H NMR (600 MHz, $CDCl_3$) δ 7.72 (bs, 1H, NH), 5.90 (d, J = 10.2 Hz, 2H), 5.31 (t, J = 9.3 Hz, 2H), 5.16 (t, J = 9.9 Hz, 2H, C$\underline{H}_2$), 5.11–5.07 (m, 2H, C$\underline{H}_2$), 4.27–4.26 (d, J = 4.8 Hz, 1H), 4.25–4.24 (d, J = 4.8 Hz, 1H), 4.14–4.13 (d, J = 2.4 Hz, 1H), 4.12–4.11 (d, J = 2.4 Hz, 1H), 3.87–3.84 (m, 2H), 2.03 (d, J = 7.2 Hz, 12H, OAc), 2.09 (s, 12H, OAc); ^{13}C NMR (150 MHz, $CDCl_3$) δ 170.6, 170.3, 169.4, 169.3, 164.9 (C=O), 134.6 (C=C), 79.7, 75.9, 73.8, 70.5, 67.9 (CH), 61.6 (CH_2), 20.7, 20.6, 20.5 (CH_3); HRMS (ES^+) *m/z* calculated for $C_{32}H_{39}NO_{20}S_2$-H $(M-H)^+$ 820.1428, found 820.142.

Synthesis of Fp-DTM-Gluc

Thioglucose tetraacetate (87.3 mg, 0.24 mmol) and NaOAc (19.6 mg, 0.24 mmol) were dissolved in MeCN (6 mL) and **Fp-DBM** (91.6 mg, 0.22 mmol) was added in MeCN (6 mL). The reaction mixture was stirred at room temperature for 1.5 h at room temperature then thioglucose tetraacetate (87.3 mg, 0.24 mmol) and NaOAc (19.6 mg, 0.24 mmol) were added. The reaction mixture was stirred for 10 min then MeCN was removed *in vacuo* and the residue was diluted in CH_2Cl_2 (20 mL) and H_2O (20 mL). The aqueous layer was extracted with CH_2Cl_2 (3 × 30 mL) and the combined organic layers were dried over anhydrous Na_2SO_4. The crude material was further purified by flash chromatography on silica gel (CH_2Cl_2/MeOH 99 : 1) to afford **Fp-DTM-Gluc** as a yellow solid (0.17 g, yield 80%). ^{1}H NMR (600 MHz, $CDCl_3$) δ 5.86 (d, J = 10.2 Hz, 2H), 5.31–5.28 (t, J = 9.3 Hz, 2H), 5.15–5.11 (m, 2H + 5H, Cp), 5.06–5.03 (m, 2H), 4.29 (d, J = 4.8 Hz, 1H), 4.28 (d, J = 4.8 Hz, 1H), 4.12 (d, J = 1.8 Hz, 1H), 4.10 (d, J = 1.8 Hz, 1H), 3.89–3.87 (m, 2H), 2.07 (d, J = 7.2 Hz, 12H, OAc), 2.05 (s, 6H, OAc), 2.02 (s, 6H, OAc); ^{13}C NMR (150 MHz, $CDCl_3$) δ 212.5 (C≡O), 177.0, 170.3, 169.8, 169.3, 169.2 (C=O), 137.6 (C=C), 85.1 (Cp), 80.5, 75.8, 73.8, 70.6, 68.0 (CH), 61.7 (CH_2), 20.5, 20.4, 20.3 (CH_3); HRMS (ES^+) *m/z* calculated for $C_{39}H_{43}FeN_1O_{22}S_2Na$ $(M + Na)^+$ 1020.0965, found 1020.0955, calculated for $C_{39}H_{43}FeN_1O_{22}S_2H$ $(M + H)^+$ 998.1146, found 998.1136.

Conjugation of insulin with DBM

Solutions of HCl, NaOH and NaPB were degassed before use. Insulin (5.2 mg, 0.907 μmol) was dissolved in 0.01 M HCl (0.520 mL), then 0.1 M NaOH (0.01 mL) and 100 mM sodium phosphate buffer pH 7.8 (NaPB, 0.520 mL) were added. To 0.95 mL of this solution (0.689 μmol insulin) a freshly prepared solution of TCEP (10 mM in 100 mM NaPB, 0.086 mL, 1.25 eq.) was added and the reaction mixture was stirred at room temperature for 40 min. Then **DBM** (20 mM in CH_3CN, 0.0345 mL, 1.0 eq.) was added and the reaction mixture was stirred for 10 min at room temperature. Addition of **DBM** was repeated 4 times, every 10 min, 5 times in total. After 50 min, the reaction mixture was diluted with $AcONH_4$ (20 mM, 4 mL) and purified by ultrafiltration using Amicon Ultra concentrator (3 kDa cutoff) in 20 mM $AcONH_4$ (5 mL at each cycle). 4 concentration-dilution cycles were sufficient to remove excess reagents (UV monitoring) and for buffer exchange. The purified and concentrated solution (final volume 0.410 mL) was then analyzed by UV, fluorescence and LC-ESI-MS to confirm the conjugation.

Conjugation of insulin with Fp-DBM

Solutions of HCl, NaOH and NaPB were degassed before use. Insulin (5.2 mg, 0.907 μmol) was dissolved in 0.01M HCl (0.520 mL), then 0.1 M NaOH (0.01 mL) and NaPB (0.520 mL) were added. To 0.95 mL of this solution (0.680 μmol insulin) a freshly prepared solution of TCEP (10 mM in NaPB, 0.085 mL, 1.25 eq.) was added and the reaction mixture was stirred at room temperature for 40 min. Then **Fp-DBM** (20 mM in CH_3CN, 0.034 mL, 1.0 eq.) was added and the reaction mixture was stirred for 10 min at room temperature in the dark (precipitation of **Fp-DBM** was observed after the 2nd addition, conversely to DBM). Addition of **Fp-DBM** was repeated 4 times, every 10 min, 5 times in total. After 50 min the reaction mixture was filtered on a syringe filter (PES, 0.22 μm) and the filter was rinsed with 20 mM $AcONH_4$ (1 mL). Solutions were combined, diluted with 20 mM $AcONH_4$ (3 mL) and purified by ultrafiltration using Amicon Ultra concentrator (3 kDa cutoff) in 20 mM $AcONH_4$ (5 mL at each cycle). 4 concen-

tration-dilution cycles were sufficient to remove excess reagents (UV monitoring) and for buffer exchange. The purified and concentrated solution (final volume 0.335 mL) was then analyzed by UV, fluorescence, IR and LC-ESI-MS, to confirm the conjugation.

Crystal structures determination

Single crystals of $C_{16}H_{21}N_3O_8S_2$ [**DTM-Cys**] (colorless needle) and $C_{32}H_{39}NO_{20}S_2$ [**DTM-Gluc**] (yellow needle) were mounted on a nylon loop and subjected to X-ray diffraction experiment on SuperNova, dual source diffractometer using, Cu Kα radiation and a HyPix detector. The crystals were kept at 100 K during data collection. Data reductions were performed with CrysAlisPro.[26] Multi-scan absorption correction was applied using spherical harmonics with SCALE3 ABSPACK algorithm. The structure of **DTM-Cys** was solved in Olex2[27] with the olex2.solve[28] structure solution program (Charge Flipping), and structure of **DTM-Gluc** was solved with SHELXT[29] (Intrinsic Phasing). Both structures were refined with the SHELXL refinement package[29] using Least Squares minimization.

For both structures, the H-atom positions were identifiable from the difference Fourier map but were refined with distances restrained to standardized values and the atomic displacement parameters (ADP-s) of H atoms were restrained as 'riding' on the displacement parameters of the covalently bound non-H atoms. In the case of **DTM-Cys**, H-atoms directly involved in H-bonding were freely refined. A disordered hexane molecule was observed in the structure of **DTM-Gluc**, along with few disordered acyl groups. Restrains used for refinement of these 'disordered acyl groups' refer to the unification of C–C and C–O bond lengths and angles and constraints of displacement parameters in the most disordered parts. These acyl groups were treated as rigid fragments. Two hexane molecules per unit cell were refined whereas the remaining 3 hexane molecules were disordered, so these had to be modeled using solvent masks during refinement. Information regarding solvent masks is given in Table S2 and Fig. S6. For two acyl groups lying close to disordered solvent, the ADP could not be reliably refined and were kept unrefined with the averaged reasonable values.

Biological studies

Cells. The triple-negative breast cancer cell line MDA-MB-231 (ATCC, American Type Culture Collection, Manassas, VA, USA) was cultured in Dulbecco's Modified Eagle's medium (DMEM) (Corning Life Sciences, Corning, NY, USA), supplemented with 10% fetal bovine serum (FBS) (Gibco, Grand Island, NY, USA) and 1% penicillin/streptomycin antibiotics (Gibco, Grand Island, NY, USA). Cells were maintained at 37 °C in a humidified atmosphere of 5% CO_2.

MTT assay. Cells were seeded in 96-well flat-bottom plates (SPL Life Science, Gyeonggi-do, Korea) at a density of 10 000 cells per well. The following day, they were treated with the test compounds at concentrations ranging from 1 μmol L^{-1} to 50 μmol L^{-1}. After 24 h of incubation, a freshly prepared 1 mg mL^{-1} solution of thiazolyl blue tetrazolium bromide (MTT) (Sigma-Aldrich, Merck KGaA, Darmstadt, Germany) in PBS was mixed (1 : 1) with fresh DMEM medium, achieving a final MTT concentration of 0.5 mg mL^{-1}. The medium was then replaced with this solution, and cells were incubated for 2 h at 37 °C in 5% CO_2. Following incubation, the medium was removed, and 100 μL of DMSO was added to each well to dissolve the formazan crystals, which formed as a result of MTT transformation by succinate dehydrogenase in the metabolically active mitochondria of viable cells. The absorbance A of the resulting solutions was measured using a SpectraMax i3 microplate reader (Molecular Devices, San Jose, CA, USA) at λ = 580 nm, with background correction at λ = 720 nm. The percentage of cell viability was calculated using the following formula:

$$\%\,\text{cell viability} = \frac{\left(A_T^{580} - A_T^{720}\right)}{\left(A_C^{580} - A_C^{720}\right)} \times 100$$

where A_C is the absorbance of the control sample (cells not treated) and A_T is the absorbance of the test sample.

The IC_{50} values determined as the mean of at least four independent experiments were calculated by 4-parameter logistic regression analysis of data according to the following equation:

$$\%\,\text{cell viability} = d + \frac{a - d}{1 + \left(\frac{(\text{sample})}{c}\right)^b}$$

where a is the minimum % cell viability; d is the maximum % cell viability, c is the IC_{50} and b is Hill's slope.

Cellular imaging by confocal microscopy

Confocal microscopy was used to assess the uptake of compounds by MDA-MB-231 cancer cells. Cells were seeded in a μ-Slide 8 Well Glass Bottom chamber (Ibidi GmbH, Gräfelfing, Germany) at a density of 10 000 cells per well. The following day, the cells were treated with the compounds at a concentration of 15 μmol L^{-1} and incubated for 2 h. After incubation, the culture medium containing the compounds was removed, and the cells were washed with sterile PBS before being immediately visualized with a confocal microscope. Analysis was performed using a DMI 6000 CS inverted microscope equipped with a TCS SP8 confocal system, operated by LAS 2.0.215022 software (Leica Microsystems, Wetzlar, Germany). Observations were conducted using an HC PL APO CS2 63×/1.40 oil immersion objective. Based on a lambda scan at an excitation wavelength of 405 nm, with emission readings taken every 20 nm within the wavelength range of 415–780 nm, the fluorescence peak of the compounds in cells was determined, and the detection range for further studies was established. The excitation and emission wavelength parameters were standardized for both the control material and samples stained with the tested compounds. To visualize the fluorescence of the compounds, a 405 nm UV diode laser was used for excitation, while emission was captured within the 450–600 nm wavelength range using a conventional photomultiplier tube (PMT) detector. Additionally, transmitted light was recorded with a PMT detector, enabling bright-field imaging.

To quantify fluorescence intensity in individual cells incubated with the tested compounds, at least two fields of view containing a minimum of 10 cells were analyzed. Confocal images were processed using Leica Application Suite Advanced Fluorescence 4.0.0.11706 (Leica Microsystems, Wetzlar, Germany).

Statistical analysis

The samples were compared using a *t*-Student test with a 95% confidence interval.

Results and discussion

Reaction of bromo- and dibromomaleimides with cysteine derivative

Reaction of **Fp-BM** and **Fp-DBM** with *N*-acetyl cysteine methyl ester (***N*-AcCysOMe**) was first investigated (Scheme 1). Reaction of **Fp-BM** with 1.1 equiv. of ***N*-AcCysOMe** in the presence of sodium acetate gave the substitution product **Fp-TM-Cys** in good yield. The shelf life of this adduct happened to be limited with decomposition occurring over time. Increasing the amount of ***N*-AcCysOMe** to 2.6 equiv. afforded the dithiosuccinimide **Fp-DTS-Cys** by bromide substitution and addition to the double bond in nearly quantitative yield as a mixture of *trans* and *cis* diastereoisomers in 7 : 3 ratio that were separated by silica gel column chromatography. The 2 diastereoisomers showed distinctly different ^{1}H NMR chemical shifts and patterns for the 2 protons of the succinimide ring with the *trans* diasteroisomer giving 2 singlets at 3.47 and 3.51 ppm and the *cis* isomer giving two doublets at 4.08 and 4.00 ppm. Reaction of **Fp-DBM** with 3 equiv. ***N*-AcCysOMe** afforded the dithiomaleimide **Fp-DTM-Cys** in good yield.

Reaction of the organic analogs **BM** and **DBM** with ***N*-AcCysOMe** was next examined for comparison (Scheme 2). Reaction of **BM** and 1.1 equiv. ***N*-AcCysOMe** gave the thiomaleimide **TM-Cys** in excellent yield that happened to be stable conversely to the organometallic analog **Fp-TM-Cys** (*vide supra*). Finally, reaction of **DBM** with 2.2 equiv. ***N*-AcCysOMe** gave **DTM-Cys**. Interestingly, among all the reaction products, only **DTM-Cys** showed bright blue-greenish fluorescence under the UV lamp (Fig. S1), in agreement with the literature[15] while the organometallic analog **Fp-DTM-Cys** was non emissive (see below).

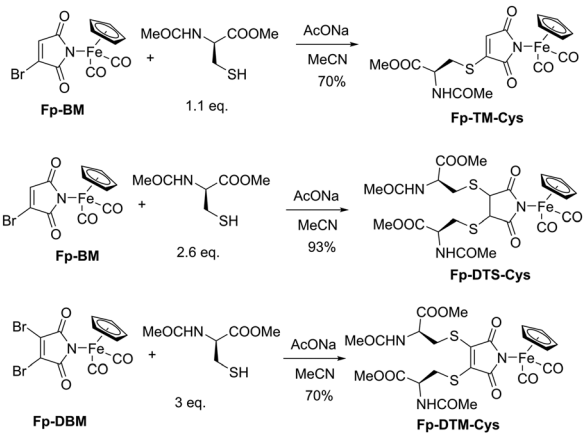

Scheme 1 Reaction of **Fp-BM** or **Fp-DBM** with ***N*-AcCysOMe**.

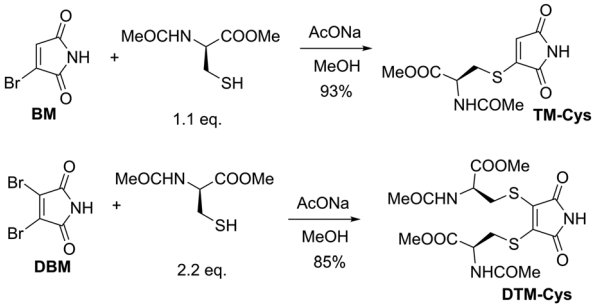

Scheme 2 Reaction of (i) bromomaleimides **BM** and **DBM** with ***N*-AcCysOMe**.

Reaction of dibromomaleimides with thioglucose derivative

As an alternative to the amino acid cysteine, we were also interested in appending a sugar moiety to the maleimide scaffold in the purpose to promote the compounds uptake by cancer cells *via* glucose transporters. To this aim, we chose 1-thio-β-D-glucose tetraacetate as this compound has already been associated to different transition metal complexes either as a S-ligand as in auranofin and related gold compounds, or appended to ligands coordinating iridium,[30–32] rhenium or technetium.[33] Reaction of 2.1 equiv. of 1-thio-β-D-glucose tetraacetate with **DBM** or **Fp-DBM** afforded the expected conjugates **DTM-Gluc** and **Fp-DTM-Gluc** in excellent yield (Scheme 3). Similarly to **DTM-Cys**, **DTM-Gluc** showed blue-green fluorescence under the UV lamp (Fig. S1) while **Fp-DTM-Gluc** was non emissive.

Spectroscopic characterization of conjugates

The monosubstituted derivatives **TM-Cys** and **Fp-TM-Cys** displayed quite similar ^{1}H NMR chemical shifts and patterns although their spectra were recorded in two different solvents (Fig. S14 and S18). The methylene protons α to the sulfur atom were diastereotopic as they showed distinct chemical shifts and a doublet of doublets pattern. Regarding the disubstituted maleimides, the methylene protons of **DTM-Cys** displayed two doublets of doublets with different ^3J coupling constants with HC(NHAc)(CO_2Me), suggesting a rigid conformation brought by steric hindrance and hydrogen bonding as shown by the

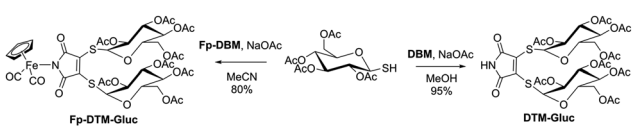

Scheme 3 Reaction of **Fp-DBM** and **DBM** with 1-thio-β-D-glucose tetraacetate.

X-ray structure (Fig. S16). On the other hand, its Fp analog (**Fp-DTM-Cys**) displayed only a doublet accounting for the four methylene protons, meaning that the presence of the Fp moiety induced a conformation in which the methylene protons lost their distinctive chemical shifts and became equivalent (Fig. S22). Furthermore, the protons on the asymmetric carbon of the two **Cys** moieties had the same chemical shift and gave a triplet of doublets for **DTM-Cys** and a doublet of triplets for **Fp-DTM-Cys**. Conversely, in **Fp-DTS-Cys**, these two protons showed distinct chemical shifts, for both *cis* and *trans* diastereoisomers (Fig. S20 and S21).

Uv-visible spectra of bromo- and dibromomaleimides and their cysteine conjugation products were recorded in MeCN (Table 1 and Fig. S2).

Fp-BM and **Fp-DBM** both display a broad absorption band at *ca.* 370 nm, common to all Fp derivatives.[34] The absorption spectra of bromo- or dibromomaleimides underwent dramatic changes upon reaction with ***N*-AcCysOMe** and 1-thio-β-D-glucose tetraacetate with DTM derivatives displaying an absorption band between 380 and 400 nm characteristic of dithiomaleimides.[15] The IR spectrum of the Fp conjugates **Fp-BM-Cys**, **Fp-DTS-Cys**, **Fp-DTM-Cys** and **Fp-DTM-Gluc** displays two bands at 2045 and 1995 cm^{-1} assigned to the stretching vibrations of the two carbonyl ligands coordinating iron.

Solutions of **DTM-Cys** in MeCN, MeOH and water were mildly fluorescent with emission maxima at 501, 527 or 550 nm, respectively (Fig. S3) demonstrating solvatochromic properties. The quantum yield of **DTM-Cys** was equal to 0.04 in MeCN. More interestingly, **DTM-Gluc** in solution in MeCN was strongly fluorescent with an emission maximum at 494 nm (Fig. S3) and a quantum yield of 0.12. As mentioned above, neither **Fp-DTM-Cys** nor **Fp-DTM-Gluc** were emissive, most likely owing to the heavy atom effect of the Fp moiety appended to the dithiomaleimide ring. However, we observed a slow increase of emission over time both in MeCN and PBS, consistent with their progressive decomposition and formation of the organic derivatives **DTM-Cys** and **DTM-Gluc** (Fig. S4).

Molecular structures

DTM-Gluc and **DTM-Cys** crystallized in chiral space groups $P2_1$ and $P2_12_12_1$ respectively. Experimental analysis confirms that all molecules in each crystal structure exhibit the same chirality, with opposite configurations in the two crystals (see Table S1 for details). Structure of disubstituted maleimide ring is conserved in both compounds. Bond lengths and angles are very similar (Table S5) and only the Cx–S-ring torsion angles differ between these two structures from 170°–180° in **DTM-Gluc** to 140° in **DTM-Cys** (Fig. S8).

DTM-Gluc crystallized with 6 independent molecules in the asymmetric unit (a representative molecule is shown in Fig. 2) with approximately 5 solvent molecules in structural voids. Strong N–H···O hydrogen bonds, classified as D1,1(2) according to M. Etter notation,[35] connect molecules into dimers (Fig. S5a and Table S3). However, the second of the two acetylated thioglucose fragments (denoted L in Fig. 2) does not participate in dimer formation and is thus more labile, with atomic positions more difficult to determine.

In contrast, **DTM-Cys** crystallized with only one independent molecule and no traces of solvent. The two amino acid fragments in the molecule arrange analogously to an antiparallel protein β-sheet (Fig. 3a and Table S4), stabilized by two short intramolecular H-bonds (C1,1(10) motif according to Etter notation[35]). These chains arrange as long columns along the [010] direction (Fig. S7).

Stability in aqueous medium

Both dibromomaleimides and dithiomaleimides are prone to hydrolysis in aqueous medium, leading to ring opening to maleamic acids.[13] In both cases, the rate of hydrolysis happens to depend on the nature of the substituent on the N

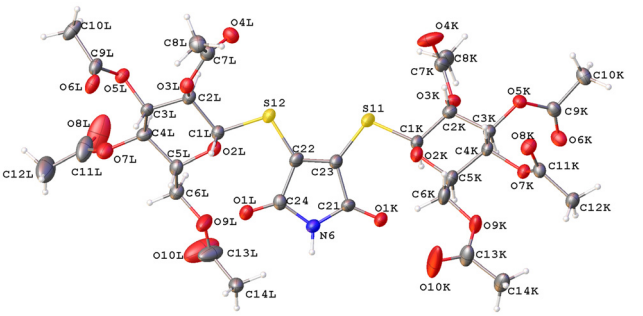

Fig. 2 Molecular structure of **DTM-Gluc**. Naming scheme for 6-th from 6 independent molecules from asymmetric unit. Sulfur atoms are named from S1 to S12, nitrogens from N1 to N6, carbons from maleimide ring are named without subscript and carbon and oxygen atoms from thioglucose moieties are named with subscript from A to L (*e.g.* S12 – subscript L, S1 subscript A). Atomic displacement parameters are represented at 50% probability level.

Table 1 Electronic absorption spectroscopy of bromo- and dibromomaleimides and their cysteine and thioglucose conjugates in MeCN

Compound	λ_{max} (nm)	ε (L mol^{-1} cm^{-1})	Compound	λ_{max} (nm)	ε (L mol^{-1} cm^{-1})
Fp-BM	369	730	**BM**	277	270
Fp-DBM	367	830	**DBM**	303	1910
Fp-TM-Cys	Unstable		**TM-Cys**	340	3370
Fp-DTS-Cys	No λ_{max}				
Fp-DTM-Cys	386	4260	**DTM-Cys**	394	3340
	308	12 840			
Fp-DTM-Gluc	387	1450	**DTM-Gluc**	371	3020
	312	5850		250	6200

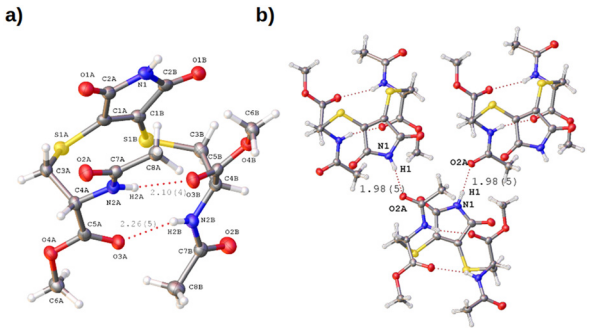

Fig. 3 Molecular structure of **DTM-Cys**: (a) the applied numbering scheme; H atom numbers are the same as those of the closest covalently bound C atom, (b) the H···O intramolecular distances displayed in Å. Atomic displacement parameters represented at 50% probability level.

of the maleimide ring. We monitored the stability of the dibromomaleimides and dithiomaleimides in PBS pH 7.4 by absorption spectroscopy (Fig. S9). The UV-vis spectrum of **DBM** evolved with time with a progressive disappearance of the peak at 243 nm. Its half-life was estimated to 94 min. On the other hand, no significant evolution of the absorption spectrum of **Fp-DBM** was observed over 24 h in the dark. The same trends were noticed for the DTM derivatives with a slow change of the UV-vis spectra of **DTM-Cys** and **DTM-Gluc** over 150 min and no change of the UV-vis spectra of **Fp-DTM-Cys** and **Fp-DTM-Gluc** over 24 h in the dark. This indicated that attachment of Fp moiety to the nitrogen of the maleimide ring efficiently protected both the dibromo- and dithiomaleimides from hydrolysis.

Reaction of dibromomaleimides with bovine insulin

It was previously reported that the sole disulfide bridge of the 32-amino acid peptide salmon calcitonin could be efficiently rebridged by reaction of **DBM** after reduction with TCEP.[9,15] We thus examined whether **DBM** or **Fp-DBM** would also be able to rebridge a disulfide bridge in another small protein, namely insulin. Bovine insulin contains 3 disulfide bridges (1 intrachain A, 2 interchain, Fig. S10) and according to the literature, the most solvent accessible disulfide bond is the one between Cys20 of chain A and Cys10 of chain B.

Insulin was first treated with TCEP (1.25 equiv.) at pH 7.8 for 15 or 40 min then 1 equiv. **Fp-DBM** or **DBM** was added every 10 min over 50 min. Of note, precipitation was observed after addition of the second equivalent of **Fp-DBM** conversely to **DBM**, likely because of its lower solubility in the buffer. After 1 h, the protein conjugates **Fp-DTM-Ins** and **DTM-Ins** were purified by ultrafiltration and analyzed by UV-visible, IR and fluorescence spectroscopy as well as by LC/ESI-MS. The UV-visible spectra of **Fp-DTM-Ins** and **DTM-Ins** strongly resembled those of the corresponding cysteine and thioglucose conjugates with a broad absorption band around 400 nm and a peak at 320 nm for **Fp-DTM-Ins** while **DTM-Ins** showed an intense absorption at 393 nm (Fig. S10).

As expected, the solution of **DTM-Ins** was noticeably fluorescent with an emission maximum at 517 nm (Fig. S10). The position of the emission band of the DTM fluorophore was significantly blue shifted compared to **DTM-Cys**, indicating that the protein provided a lipophilic environment to the dithiomaleimide group. On the other hand, the IR spectrum of **Fp-DTM-Ins** showed 2 typical νCO band at 2050 and 2000 cm^{-1} (Fig. 4, panel D), characteristic of the Fp motif.

The intact protein conjugates were also analyzed by LC/ESI-MS. The deconvoluted mass spectrum of **DTM-Ins** showed 3 to 4 major peaks (Fig. 4 and Table 2) assigned to unmodified insulin and conjugates containing 1, 2 or 3 DTM entities. The percentage of peak intensities of the protein conjugates depended on the reduction step duration. For instance, the peak at 5831 Da corresponding to the monoconjugate accounts for 17.5% of the unmodified protein when the reduction time is 10 min while it only accounts for 3.6% of the of the unmodified protein when the reduction time is 40 min. In contrast, the relative proportion of the diconjugate raised from 13.5% to 20% with increasing reduction time from 10 to 40 min. The deconvoluted mass spectrum of **Fp-DTM-Ins** also displayed a series of peaks in addition to that of unmodified insulin at 5739 Da, assigned to conjugates with 1 or 2 Fp-DTM entities.

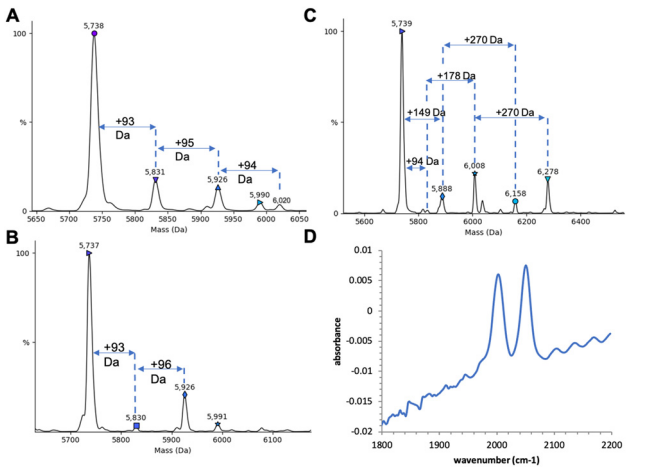

Fig. 4 Deconvoluted ESI-MS mass spectra of **DTM-Ins** (A and B) and **Fp-DTM-Ins** (C); the spectrum of **DTM-Ins** shown in panel A was obtained using a 15 min reduction time while the spectra of **DTM-Ins** and **Fp-DTM-Ins** shown in panels B and C were obtained using a 40 min reduction time. IR spectrum of **Fp-DTM-Ins** (D).

Table 2 ESI-MS of **DTM-Ins** and **Fp-DTM-Ins**; peaks assignment

DTM-Ins		**Fp-DTM-Ins**	
m (Da)	Assignment	*m* (Da)	Assignment
5738	Insulin	5739	Insulin
5831	Insulin + 1 DTM	5888	Insulin + 1 Fe-DTM
5926	Insulin + 2 DTM	6008	Insulin + 1 Fp-DTM
5990 or 5991	Not assigned	6158	Insulin + 2 Fe-DTM
6020	Insulin + 3 DTM	6278	Insulin + 2 Fp-DTM

Light irradiation experiments

Visible light irradiation of a solution of **Fp-DTM-Cys** and **Fp-DTM-Gluc** in MeCN qualitatively induced a change of their absorption spectra with the appearance of a band at *ca.* 400 nm and the simultaneous disappearance of the band at *ca.* 310 nm (Fig. S11). Moreover, the fluorescence spectra of solutions of **Fp-DTM-Gluc** and **Fp-DTM-Cys** showed a broad emission band centered at 490 or 515 nm after 3 or 4 h irradiation at 370 nm. These two results are consistent with the conversion of these conjugates to **DTM-Cys** and **DTM-Gluc** (Scheme 4).

Still, to unambiguously identify the photoproduct, a ^{1}H NMR experiment was performed in parallel, where **Fp-DTM-Gluc** in solution in CD_2Cl_2 was irradiated for up to 96 h with visible light (Fig. 5). Progressive disappearance of the singlet at 5.15 ppm assigned to the 5 protons of the Cp ligand was observed along with the appearance of a singlet at 7.7 ppm assigned to the proton of the maleimide ring. No significant changes were noticed for the other peaks. Thus, this experiment confirmed that irradiation of **Fp-DTM-Gluc** results in the decomposition of the Fp motif upon photoexcitation[22,36] and subsequent formation of **DTM-Gluc**. As already reported, Fp-imidato complexes release 2 CO, iron(III) species, CpH and imide upon irradiation with visible light.[22,36]

Fp-DTM-Ins was also irradiated under similar conditions, and a broad emission band centered at 519 nm was again observed after 2 h which confirmed the formation of **DTM-Ins** upon decomposition of the Fp entity (Fig. S11). The fluorescence of formed **DTM-Ins** provided indirect evidence for the previous formation of **Fp-DTM-Ins** upon reaction of **Fp-DBM** with insulin.

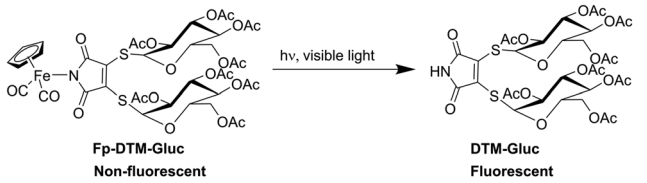

Scheme 4 Irradiation of **Fp-DTM-Gluc** with visible light.

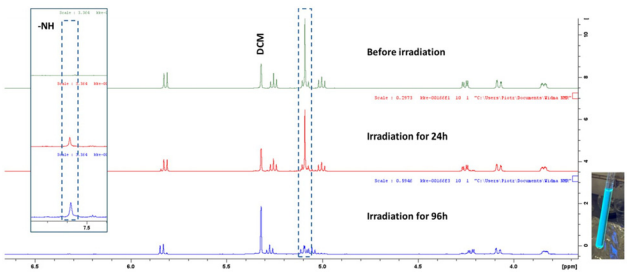

Fig. 5 ^{1}H NMR spectra of **Fp-DTM-Gluc** in CD_2Cl_2 before and after irradiation with visible light. Photo of NMR tube under UV lamp taken after 96 h of irradiation.

Biological studies

In a previous article, some of us had reported that **FpM** was mildly cytotoxic to human promyelocytic leukemia cells, both in the dark and after illumination,[23] likely due to its ability to react with biological thiols along with its CO releasing property. Indeed, complexes Fp-X (X = Cl, Br, I) have long been known to spontaneously release CO in the dark with half-lives ranging from 150 to 350 min at 37 °C according to the myoglobin assay.[37] Visible light irradiation strongly accelerates the CO release process with half-lives of 67 min for **FpM** and 48 min for its succinimide analog.[22]

The effect of the (di)bromomaleimides and the cysteine and thioglucose conjugates on the viability of "triple negative" breast cancer cells MDA-MB-231 was first examined. Cells were exposed to 5 different concentrations of each compound in the dark and cell viability was measured by the colorimetric MTT assay after 24 h to determine their IC_{50} value, defined as the concentration for which cell viability is reduced by 50% relative to control (Table 3). To our delight, **Fp-DBM**, **Fp-BM** and **Fp-DTM-Gluc** induced a concentration-dependent decrease of cell viability (Fig. S12). Conversely, **DBM** and the two organic dithiomaleimides **DTM-Cys** and **DTM-Gluc** as well as **Fp-DTM-Cys** were non toxic to MDA-MB231 cells in the tested conditions.

We hypothesize that the cytotoxicity of **Fp-DTM-Gluc** could arise from the Fp entity and its ability to release CO since the organic analog is non toxic. The presence of the Gluc entities could also favor its cell uptake since **Fp-DTM-Cys** was unable to decrease the viability of MDA-MB-231 cells up to 50 μM. Although both **DBM** and **Fp-DBM** are highly reactive toward thiols which may affect cell functioning, only **Fp-DBM** was found cytotoxic, illustrating again the contribution of the Fp group that favors cell uptake and prevents the rapid hydrolysis of the maleimide ring. The same arguments likely hold true for **Fp-BM** although the organic analog has not been tested for comparison.

MDA-MB-231 cells were next exposed to 15 μM of each compound for 2 h in the dark and fluorescence and transmission images of the cells in the green channel were taken with a confocal microscope (Fig. 6). Excitation and emission parameters were standardized for both the control sample and the samples incubated with the tested compounds.

Relatively weak intracellular fluorescence signal was detected in cells incubated with **DTM-Gluc**, **DTM-Cys**, **Fp-DTM-Cys** and **DBM**, with the signal originating mainly from oval and granular structures, most likely mitochondria. In contrast, cells incubated with **Fp-BM** exhibited a diffuse cyto-

Table 3 IC_{50} values of selected compounds on MDA-MB-231 breast cancer cells after 24 h-incubation

Compound	IC_{50} (μM)
Fp-DBM	8.4 ± 1.5
Fp-BM	10.5 ± 0.5
Fp-DTM-Gluc	17.4

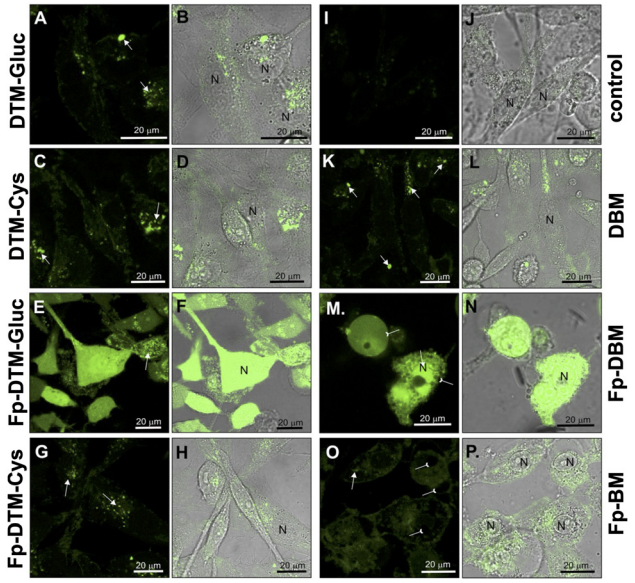

Fig. 6 Confocal microscopy images showing the intracellular localization of tested compounds at 15 µM concentration in living MDA-MB-231 cells after 2 h-incubation. Ex/em: 405/450–600 nm. Fluorescence images are presented in panels A, C, E, G, I, K, M and O; corresponding merged images (fluorescence + transmitted light) are shown in panels B, D, F, H, J, L, N and P. Arrows indicated a fluorescent granular pattern, while inverted arrows highlight swollen, bubbling cells.

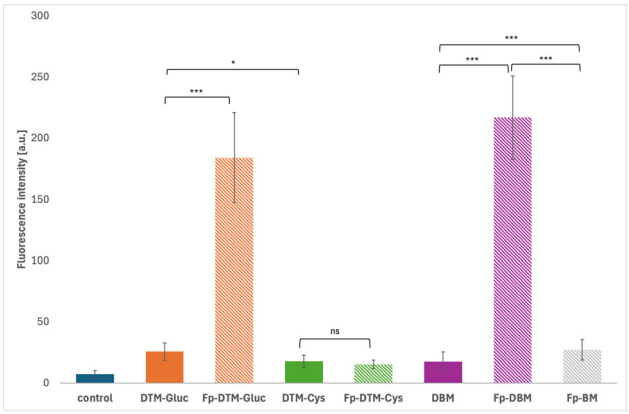

Fig. 7 Quantitative comparison of fluorescence intensity of MDA-MB-231 breast cancer cells exposed for 2 h with 15 µM of the tested compounds. Excitation/emission: 405/450–600 nm. ROI = 20. Measurements were extracted from the original confocal datasets. For each compound, ≥2 fields of view comprising ≥10 cells each were analyzed; data are mean ± SD. ns: $p > 0.05$; *: $0.01 < p < 0.05$; ***: $p < 0.001$.

plasmic fluorescence and cells treated with **Fp-DTM-Gluc** and **Fp-DBM** displayed a very intense fluorescence signal with a maximum at *ca.* 520 nm (Fig. S13), and a staining pattern that primarily involved the nucleus, cytoplasm, and mitochondria. Moreover, cells treated with **Fp-DTM-Gluc**, **Fp-DBM**, and **Fp-BM** showed pronounced alterations, mainly related to cell membrane damage, with the most severe effects observed for cells incubated with **Fp-DBM**.

Fluorescence intensity measurements in individual cells confirmed microscopic observations (Fig. 7). Cells exposed to the tested compounds displayed mean fluorescence intensities statistically different from the value of the untreated cells ($p < 0.001$), with values 2 to 4-fold higher than control for **DBM**, **DTM-Gluc**, **DTM-Cys**, **Fp-DTM-Cys** and **Fp-BM**.

The lack of emission of **DBM**, **Fp-DTM-Cys** and **Fp-BM** in solution may explain the weak fluorescence of cells exposed to these compounds. The poor fluorescence intensity of cells exposed to **DTM-Gluc** is more surprising since this compound is highly fluorescent in solution (see above). The inability of this compound to cross the cell membrane may account for this discrepancy. On the other hand, the level of fluorescence in cells treated with **Fp-DTM-Gluc** and **Fp-DBM** was 25–30 times higher than control, even though both compounds are non emissive in solution. Therefore, they must have undergone chemical transformations inside cells to explain this finding. For **Fp-DTM-Gluc**, intracellular fluorescence most likely results from the loss of the Fp moiety after 2 h, leading to fluorescent **DTM-Gluc**. This indicates that the Fp entity rather than the glucose entities favors cell uptake since cells treated with **DTM-Gluc** are poorly fluorescent. For **Fp-DBM**, a plausible explanation is that it is converted to a DTM derivative in cells (for instance by reaction with GSH present in millimolar concentration in cancer cells)[21] with concomitant loss of its Fp entity. Here again, the presence of the Fp entity seems to promote cell uptake, since cells treated with **DBM** do not show appreciable fluorescence.

Confocal microscopy data thus provide an explanation for the biological activity of the tested compounds and the specific role of the Fp entity for cell permeation and as supplier of toxic species like CO. This makes **Fp-DBM** and **Fp-DTM-Gluc** new examples of fluorogenic CORMs, generating fluorescent species upon release of CO.[38–40] Let us note that the cell viability and the cell uptake experiments were carried out in the dark so that the loss of Fp and subsequent release of CO observed for Fp derivatives occur through a mechanism not involving light.

Conclusions

In conclusion, **Fp-BM** and **Fp-DBM** as well as **BM** and **DBM** readily react with thiols (cysteine, thioglucose derivatives) and serve as rebridging agents for a disulfide-containing protein (bovine insulin). The obtained maleimide bioconjugates **Fp-DTM-Cys**, **Fp-DTM-Gluc**, **Fp-DTM-Ins** show typical absorption bands in the mid-IR spectral range owing to the 2 carbonyl ligands but are devoid of fluorescence properties conversely to their organic analogs **DTM-Cys**, **DTM-Gluc**, **DTM-Ins** which exhibit intense fluorescence. Upon irradiation with visible light, the Fp derivatives (**Fp-DTM-Cys**, **Fp-DTM-Gluc**, **Fp-DTM-Ins**) change of spectroscopic properties from IR label to fluorescent label, due to loss of Fp entity. Because this loss is linked to the decoordination of the ligands (CO, CpH, imide)

from the metal, the release of CO can be confirmed by appearance of fluorescence, thus **Fp-DTM** derivatives could be new examples of "turn-on" Photo-CORM probes.

From the biological studies, we found that the Fp derivatives showed significant cytotoxicity toward triple negative breast cancer cells while the organic analogs were non cytotoxic. This could be explained by the presence of the Fp group that promotes cell uptake, prevents ring opening *via* hydrolysis and releases bioactive species such as CO and Fe^{3+} ion. The fluorogenic properties of **Fp-DBM** and **Fp-DTM-Gluc** proved extremely useful to provide information on their intracellular transformation as shown by confocal microscopy. Indeed, the intense fluorescence of cells exposed to these complexes indicated that they both lost the Fp group and that biological thiols bound to DBM to form DTM adducts. The effect of Fp group on biological activities of Fp-DTM derivatives appears extremely promising but their mechanism of action needs further studies.

Author contributions

K. K.: (organic synthesis & biological studies) investigation, N. F-D.: (biological studies) supervision, investigation, S. M. (cytotoxicity and confocal microscopy studies) methodology, investigation, M. G. (confocal microscopy studies) investigation, M. G: (cytotoxicity) investigation; A. M. and J. K.: (crystallography) investigation, validation, visualization; A. W. (organic synthesis) investigation, L. L.: (mass spectrometry) investigation, M. S.: conceptualization, methodology, manuscript writing; B. R.: conceptualization, methodology, supervision, manuscript writing.

Conflicts of interest

There are no conflicts to declare.

Data availability

The data supporting this article have been included as part of the supplementary information (SI). Supplementary information is available. See DOI: https://doi.org/10.1039/d5dt02375k.

(a) CCDC 2486387 (**DTM-Cys**): Experimental Crystal Structure Determination, 2025, (b) CCDC 2486281 (**DTM-Gluc**): Experimental Crystal Structure Determination, 2025.[41a,b]

Acknowledgements

This work was financially supported by the Faculty of Chemistry, University of Lodz. A. M. acknowledges the support of the National Science Centre, Poland (grant no. DEC-2021/41/B/ST4/02760). K. K. thanks the Erasmus program for funding internships at Sorbonne Université. The authors acknowledge the MS3U (Mass Spectrometry Sciences Sorbonne University, FcMol, UAR2769, CNRS and Sorbonne Université) platform for HRMS and LC-ESI-MS analysis. The authors thank Prof. Agnieszka Z. Wilczewska for the graphical abstract.

References

1 J. M. J. M. Ravasco, H. Faustino, A. Trindade and P. M. P. Gois, *Chem. – Eur. J.*, 2019, **25**, 43–59.
2 S. L. Kuan, T. Wang and T. Weil, *Chemistry*, 2016, **22**, 17112–17129.
3 N. Forte, V. Chudasama and J. R. Baker, *Drug Discovery Today: Technol.*, 2018, **30**, 11–20.
4 K. Yamada and Y. Ito, *ChemBioChem*, 2019, **20**, 2729–2737.
5 L. M. Tedaldi, M. E. B. Smith, R. I. Nathani and J. R. Baker, *Chem. Commun.*, 2009, 6583–6585.
6 M. E. B. Smith, F. F. Schumacher, C. P. Ryan, L. M. Tedaldi, D. Papaioannou, G. Waksman, S. Caddick and J. R. Baker, *J. Am. Chem. Soc.*, 2010, **132**, 1960–1965.
7 F. F. Schumacher, M. Nobles, C. P. Ryan, M. E. B. Smith, A. Tinker, S. Caddick and J. R. Baker, *Bioconjugate Chem.*, 2011, **22**, 132–136.
8 S. A. Fletcher, P. K. B. Sin, M. Nobles, E. Årstad, A. Tinker and J. R. Baker, *Org. Biomol. Chem.*, 2015, **13**, 9559–9563.
9 M. W. Jones, R. A. Strickland, F. F. Schumacher, S. Caddick, J. R. Baker, M. I. Gibson and D. M. Haddleton, *J. Am. Chem. Soc.*, 2012, **134**, 1847–1852.
10 C. M. Grison, G. M. Burslem, J. A. Miles, L. K. A. Pilsl, D. J. Yeo, Z. Imani, S. L. Warriner, M. E. Webb and A. J. Wilson, *Chem. Sci.*, 2017, **8**, 5166–5171.
11 A. Lindsey-Crosthwait, D. Rodriguez-Lema, M. Walko, C. M. Pask and A. J. Wilson, *Pept. Sci.*, 2021, **113**, e24157.
12 C. R. Behrens, E. H. Ha, L. L. Chinn, S. Bowers, G. Probst, M. Fitch-Bruhns, J. Monteon, A. Valdiosera, A. Bermudez, S. Liao-Chan, T. Wong, J. Melnick, J.-W. Theunissen, M. R. Flory, D. Houser, K. Venstrom, Z. Levashova, P. Sauer, T.-S. Migone, E. H. van der Horst, R. L. Halcomb and D. Y. Jackson, *Mol. Pharmaceutics*, 2015, **12**, 3986–3998.
13 M. Morais, J. P. M. Nunes, K. Karu, N. Forte, I. Benni, M. E. B. Smith, S. Caddick, V. Chudasama and J. R. Baker, *Org. Biomol. Chem.*, 2017, **15**, 2947–2952.
14 M. Farleigh, T. T. Pham, Z. Yu, J. Kim, K. Sunassee, G. Firth, N. Forte, V. Chudasama, J. R. Baker, N. J. Long, C. Rivas and M. T. Ma, *Bioconjugate Chem.*, 2021, **32**, 1214–1222.
15 M. P. Robin, P. Wilson, A. B. Mabire, J. K. Kiviaho, J. E. Raymond, D. M. Haddleton and R. K. O'Reilly, *J. Am. Chem. Soc.*, 2013, **135**, 2875–2878.
16 S. Kong, X. Gao, Q. Wang, J. Lin, L. Qiu and M. Xie, *Molecules*, 2023, **28**(20), 1420.
17 J. T. Husband, A. C. Hill and R. K. O'Reilly, *Polymer Int.*, 2019, **68**, 1247–1254.
18 Y. Xie, J. T. Husband, M. Torrent-Sucarrat, H. Yang, W. Liu and R. K. O'Reilly, *Chem. Commun.*, 2018, **54**, 3339–3342.
19 H. Wang, M. Xu, M. Xiong and J. Cheng, *Chem. Commun.*, 2015, **51**, 4807–4810.

20 Z. Tang, P. Wilson, K. Kempe, H. Chen and D. M. Haddleton, *ACS Macro Lett.*, 2016, **5**, 709–713.
21 B. Rudolf, M. Salmain, E. Fornal and A. Rybarczyk-Pirek, *Appl. Organomet. Chem.*, 2012, **26**, 80–85.
22 A. Kubicka, E. Parfieniuk, E. Fornal, M. Palusiak, D. Lizińska, A. Gumieniczek and B. Rudolf, *J. Photochem. Photobiol., A*, 2018, **351**, 115–123.
23 D. Wysokiński, P. Lewandowska, D. Ząták, M. Juszczak, M. Kluska, D. Lizińska, B. Rudolf and K. Woźniak, *Toxicol. Res.*, 2019, **8**, 544–551.
24 B. F. Hallam and P. L. Pauson, *J. Chem. Soc.*, 1956, 3030–3037.
25 M. T. Marty, A. J. Baldwin, E. G. Marklund, G. K. A. Hochberg, J. L. P. Benesch and C. V. Robinson, *Anal. Chem.*, 2015, **87**, 4370–4376.
26 Rigaku Oxford Diffraction, *CrysAlisPro Software system, version 1.171.38.46*, Rigaku Corporation, Oxford, UK, 2017.
27 O. V. Dolomanov, L. J. Bourhis, R. J. Gildea, J. A. K. Howard and H. Puschmann, *J. Appl. Crystallogr.*, 2009, **42**, 339–341.
28 L. J. Bourhis, O. V. Dolomanov, R. J. Gildea, J. A. K. Howard and H. Puschmann, *Acta Crystallogr., Sect. A*, 2015, **71**, 59–75.
29 G. M. Sheldrick, *Acta Crystallogr., Sect. A*, 2015, **A71**, 3–8.
30 A. Prokop, J. A. Czaplewska, M. Clausen, M. König, A. Wild, R. Thorwirth, B. Schulze, K. Babiuch, D. Pretzel, U. S. Schubert and M. Gottschaldt, *Eur. J. Inorg. Chem.*, 2016, **2016**, 3480–3488.
31 M.-J. Li, P. Jiao, W. He, C. Yi, C.-W. Li, X. Chen, G.-N. Chen and M. Yang, *Eur. J. Inorg. Chem.*, 2011, **2011**, 197–200.
32 K. Fukumoto, K. Hyakumura, Y. Sakai, S. Yano, A. Nomoto, S. Miyashita, A. Narumi and A. Ogawa, *J. Mater. Sci. Eng. A*, 2016, **6**, 283–288.
33 M. Gottschaldt, D. Koth, D. Müller, I. Klette, S. Rau, H. Görls, B. Schäfer, R. P. Baum and S. Yano, *Chem. – Eur. J.*, 2007, **13**, 10273–10280.
34 N. Fischer-Durand, M. Salmain, B. Rudolf, A. Vessieres, J. Zakrzewski and G. Jaouen, *ChemBioChem*, 2004, **5**, 519–525.
35 M. C. Etter, J. C. MacDonald and J. Bernstein, *Acta Crystallogr., Sect. B*, 1990, **B46**, 256–262.
36 A. Kosińska, S. Wojtulewski, M. Palusiak, P. Tokarz and B. Rudolf, *Organometallics*, 2021, **40**, 663–673.
37 D. Scapens, H. Adams, T. R. Johnson, B. E. Mann, P. Sawle, R. Aqil, T. Perrior and R. Motterlini, *Dalton Trans.*, 2007, 4962–4973.
38 S. J. Carrington, I. Chakraborty, J. M. L. Bernard and P. K. Mascharak, *ACS Med. Chem. Lett.*, 2014, **5**, 1324–1328.
39 D. Musib, M. K. Raza, K. Martina and M. Roy, *Polyhedron*, 2019, **172**, 125–131.
40 I. Chakraborty, S. J. Carrington, G. Roseman and P. K. Mascharak, *Inorg. Chem.*, 2017, **56**, 1534–1545.
41 (*a*) CCDC 2486281: Experimental Crystal Structure Determination, 2025, DOI: 10.5517/ccdc.csd.cc2pg5mz; (*b*) CCDC 2486387: Experimental Crystal Structure Determination, 2025, DOI: 10.5517/ccdc.csd.cc2pg91j.